ZEBRAFISH
Volume 10, Number 3, 2013

DOI: 10.1089/zeb.2013.0876

# Methotrexate-Induced Decrease in Embryonic 5-Methyl-Tetrahydrofolate Is Irreversible with Leucovorin Supplementation

Tseng-Ting Kao,[1] Gang-Hui Lee,[1] Chi-Chang Fu,[2] Bing-Hung Chen,[3] Li-Ting Chen,[2] and Tzu-Fun Fu[1,2]

## Abstract

Folate is a nutrient crucial for rapidly growing tissues, including developing embryos and cancer cells. Folate participates in the biosynthesis of nucleic acids, proteins, amino acids, S-adenosylmethionine, many neurotransmitters, and some vitamins. The intracellular folate pool consists of different folate adducts, which carry one-carbon units at three different oxidative states and participate in distinct biochemical reactions. Therefore, the content and dynamics of folate adducts will affect the homeostasis of the metabolites generated in these folate-mediated reactions. Currently, the knowledge on the level of each individual folate adduct in developing embryos is limited. With an improved high-performance liquid chromatography protocol, we found that tetrahydrofolate (THF), the backbone of one-carbon carrier, gradually increased and became dominant in developing zebrafish embryos. 5-methyl-tetrahydrofolate (5-$CH_3$-THF) was abundant in unfertilized eggs but decreased rapidly when embryos started to proliferate and differentiate. 10-formyltetrahydrofolate at first increased after fertilization, and then dropped dramatically before reaching a sustained level at later stages. Dihydrofolate (DHF) slightly decreased initially and remained low throughout embryogenesis. Exposure to methotrexate significantly decreased 5-$CH_3$-THF levels and increased DHF pools, besides causing brain ventricle anomaly. Rescuing with leucovorin partly reversed the abnormal phenotype. Unexpectedly, the level of 5-$CH_3$-THF remained low even when leucovorin was added for rescue. Our results show that different folate adducts fluctuated significantly and differentially in concert with the physiological requirement specific for the corresponding developmental stages. Furthermore, methotrexate lowered the level of 5-$CH_3$-THF in developing embryos, which could not be reversed with folate supplementation and might be more substantial to cellular methylation potential and epigenetic control than to nucleotide synthesis.

## Introduction

Folate deficiency is a malnutrition often encountered clinically and has been related to many diseases, including cancers, cardiovascular diseases, and neuropathies.[1] Deficiency of folate, or disturbance in folate-mediated one-carbon metabolism, has also been implicated in several congenital defects, including neural tube defects (NTD), one of the most common birth defects occurring in approximately one in 1000 live births in the United States and worldwide. The growing awareness on the importance of folate has increased the public demand for folate supplementation. Ample amounts of folic acid are ingested by general population, including pregnant women, as a daily nutritional supplement. Despite the well-documented beneficial effects of folate supplementation in preventing NTD,[2] detrimental effects of unmetabolized folic acid and supraphysiological folate also appear, leading to a vigorous debate on mandatory folate fortification and supplementation among researchers.[3,4] It also reveals an urgent need for further investigation on the underlying mechanism and regulation of folate-mediated one-carbon metabolism (OCM).

Folate (folic acid), also called vitamin B9, is an essential nutrient participating in the biosynthesis and metabolism of nucleic acids, proteins, amino acids, neurotransmitters, and some vitamins. Therefore, folate is vital especially for rapidly growing tissues and proliferating cells, such as fetus and cancer. Folate also plays a crucial role in epigenetic control since it provides the one-carbon unit required for S-adenosylmethionine (SAM) biosynthesis. SAM is the primary

[1]The Institute of Basic Medical Science and [2]Department of Medical Laboratory Science and Biotechnology, College of Medicine, National Cheng Kung University, Tainan, Taiwan.
[3]Department of Biotechnology, Kaohsiung Medical University, Kaohsiung, Taiwan.

methyl donor for most intracellular methylation reactions, including DNA/RNA, protein and lipid methylation. Therefore, intracellular folate content will affect gene activity, endowing folate the potential to modulate gene function simply via dietary intervention.[5] In cells, folate is both reduced to dihydrofolate (DHF) and tetrahydrofolate (THF) and polyglutamylated to form biologically active folylpolyglutamates. One-carbon units of three different oxidative states are attached to these folylpolyglutamates on either the N-5 and/or N-10 positions, forming different folate adducts (Fig. 1). These folate adducts, distributed in different cellular compartments, provide their one-carbon units to generate the biomolecules noted above.[6] The interconversion between different folate adducts also occurs via several redox and synthetic reactions catalyzed by folate enzymes. The metabolic reactions involving these pathways are referred to as OCM (Fig. 1).

The regulation for the dynamic distribution of different folate adducts during embryogenesis is important because proper folate status, including both the content and composition, at various stages of development is crucial for a normal embryogenesis. Fluctuation in the distribution of folate adducts could affect the production of biomolecules formed in OCM via changing the reaction equilibrium and direction, without altering the protein level of catalytic enzyme.[7,8] In

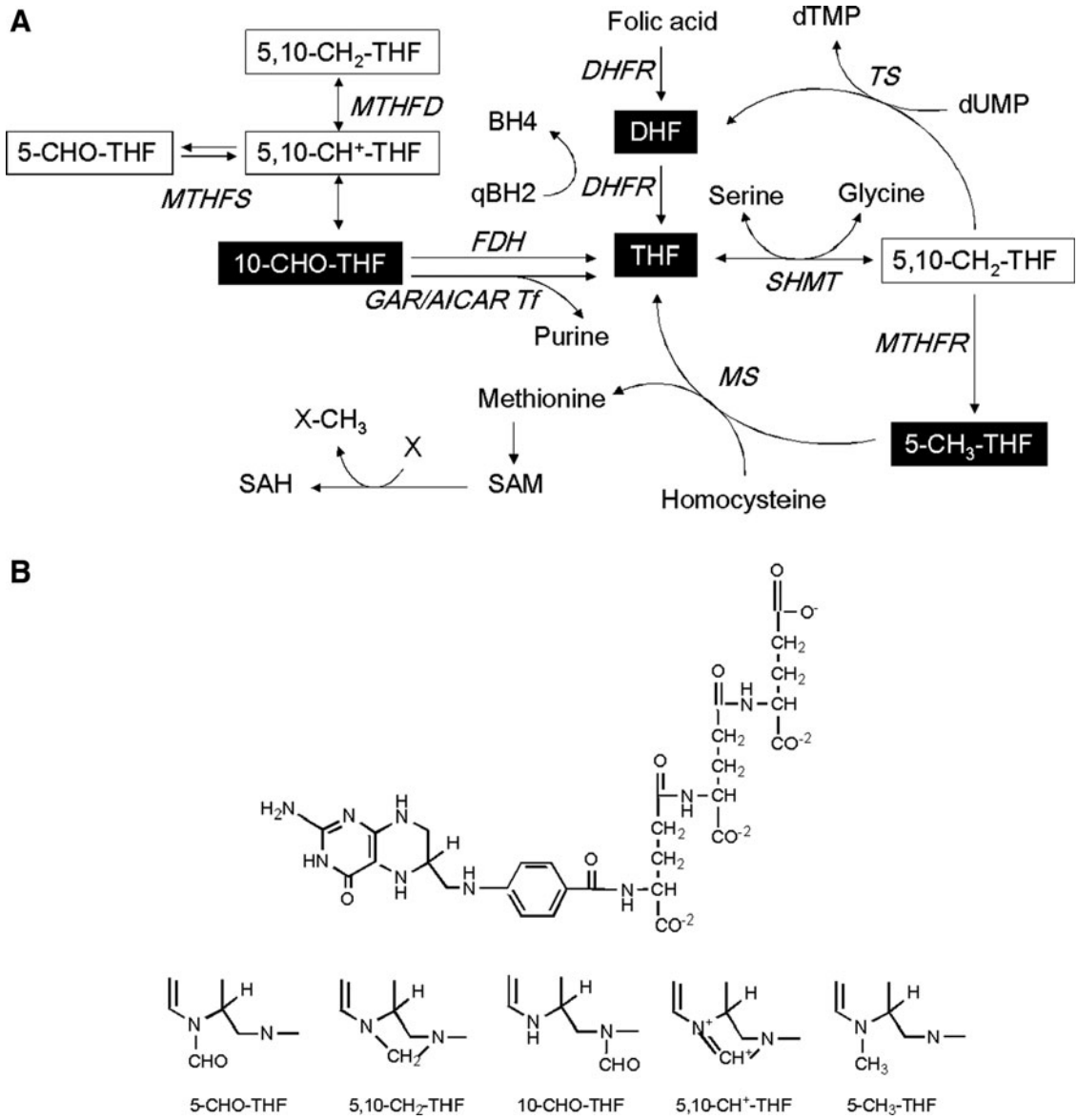


**FIG. 1.** Folate-mediated OCM and folate structure. **(A)** Reactions involving folate coenzymes and enzymes of OCM are responsible for the biosynthesis of purines, thymidylate, and SAM. The *black-boxed* compounds are folate adducts measured in the current study. MTHFD, methylenetetrahydrofolate dehydrogenase; TS, thymidylate synthase; MTHFR, methylenetetrahydrofolate reductase; MS, methionine synthase; GAR/AICAR Tf, glycinamide ribonucleotide transformylase and aminoimidazolecarboxamide ribotide transformylase; MTHFS, 5,10-methenyltetrahydrofolate synthetase; SAM, S-adenosylmethionine; SAH, S-adenosylhomocysteine; "X" denotes substances subjected to methylation. **(B)** The basic structure of tetrahydrofolate comprises a pteridine ring, a para-aminobenzoate and a polyglutamyl moiety. The number of glutamates attached to THF varies from three to nine in cells. The one-carbon group attaches to $N_5$ and/or $N_{10}$ positions. OCM, one-carbon metabolism.

general, each one-carbon adduct is important in one major pathway, that is, 5-methyl-tetrahydrofolate (5-$CH_3$-THF) in methylation of DNA and RNA, 5,10-methylene-tetrahydrofolate (5,10-$CH_2$-THF) in dTMP synthesis, and 10-formyl-tetrahydrofolate (10-CHO-THF) in purine synthesis. Since nucleotides are essential for cell proliferation and epigenetic control is crucial for cell fate determination, the knowledge on how the pools of folate adducts vary during embryogenesis and how they respond to disturbance will be important for understanding the regulation of metabolic control for folate-mediated OCM and gene activity.

Zebrafish are emerging as a prominent model organism for embryonic development and drug/toxin research because of several advantages, including ease of manipulation, transparent embryos, ease of growth and breeding, and economy.[9] More importantly, the externally fertilized and developed embryos can be viewed as a "closed system," concerning the folate-mediated one-carbon pool. This characteristic is especially important since it allows us to exclude the interference from maternal supply of folate during gestation and enable the fluctuation between different folate adducts to be observed. Moreover, many zebrafish folate enzymes have been shown to be structurally and functionally comparable to their mammalian orthologs, adding more emphasis to the appropriateness of using zebrafish to model folate-mediated OCM.[10–13]

The aim of this study is to characterize the dynamics of folate 1-C pools in developing zebrafish embryos. To accomplish our goal, we developed a new protocol for determining individual folate adducts. This protocol significantly shortens the time required for analysis and allows us to simultaneously detect different folate adducts, especially those with low stability and optical activity. In addition, we investigated the impact to embryonic OCM and embryonic development caused by methotrexate, an antifolate drug often used to treat several cancers and to induce folate deficiency in model cells or animals in laboratory. We also evaluated how the addition of leucovorin (5-CHO-THF; folinic acid is the other name) affects OCM in developing embryos. Leucovorin is the folate supplement commonly used in an antifolate combinatorial therapy to reverse the folate deficiency induced by methotrexate. The underlying mechanisms and potential clinical implication are also discussed.

## Materials and Methods

### Materials

The high-performance liquid chromatography (HPLC) Aquasil $C_{18}$ and guard columns were purchased from ThermoFisher Scientific. Nickel-Sepharose (Ni-Sepharose) resin slurry was purchased from Amersham Bioscience. All fully reduced monoglutamyl folates, except 10-CHO-THF, were generous gifts from Dr. Moser (Merck Eprova AG). 10-CHO-THF was prepared by increasing the pH of 5,10-$CH^+$-THF solution to 8.0 as previously described.[14] All other chemicals, including folic acid, DHF and buffers were purchased from Sigma-Aldrich Chemical Co.

### Preparation of zebrafish egg and embryo extracts

Zebrafish (*Danio rerio*; AB strain) were bred and maintained in a 14 h − 10 h light-dark diurnal cycle following the standard procedure.[15] Embryos were staged according to Kimmel *et al.*[16] For sample preparation, briefly, 50 zebrafish eggs, or embryos at indicated stages were collected, homogenized, and sonicated in 0.3 mL of extraction buffer flushed with nitrogen. The clear lysates were heated in boiling water for 5 min before centrifugation (Supplementary Fig. S1; Supplementary Data are available online at www.liebertpub.com/zeb). The supernatants were subjected to folate conversion and detection as stated below. The animal studies and all procedures for handling zebrafish and embryos, including breeding and maintenance of fish and sample collection, were approved by Affidavit of Approval of Animal Use Protocol of National Cheng Kung University (IACUC Approval No. 96062).

### Methotrexate and 5-CHO-THF treatments in zebrafish embryos

Embryos at 6 hour postfertilization (hpf) were moved to water containing 1.5 mM MTX with/without 5 mM 5-CHO-THF and incubated for another 6 h before embryos were collected for folate content analysis. Embryos grown in water containing no additional drug were used as controls. After removing the drug and rinsing with distilled water, embryos were manually dechorionated and subjected to folate extraction and analysis.

### Folate conversion and determination

The physiologically active forms of reduced folates have a chain of glutamate residues connected through their $\gamma$ carboxyl group. Removal of the polyglutamate portion and interconversion of one-carbon derivatives were performed following the steps depicted in Scheme 1 using several enzymes cloned, expressed, and purified as previously described. The following clones were from zebrafish: $\gamma$-glutamyl hydrolase (GGH) (Eq. 1),[17] the N-terminal domain of 10-CHO-THF dehydrogenase (FDH-N) (Eq. 2), DHF reductase (DHFR) (Eq. 3)[13], and serine hydroxymethyltransferase (SHMT) (Eq. 4).[10] FDH-N is the recombinant N-terminal domain of zebrafish FDH, which contains 10-CHO-THF hydrolase activity (Eq. 2).[12] A clone expressing *Escherichia coli FolD* gene with 5,10-methylenetetrahydrofolate dehydrogenase (MTD) activity (Eq. 5)[18] was a generous gift from Dr. Verne Schirch/Virginia Commonwealth University.

$$\text{folate-Glu}_x \rightarrow \text{folate} + \text{X Glu} \qquad \text{(Eq. 1)}$$

$$\text{10-CHO-THF} \rightarrow \text{THF} + \text{formate} \qquad \text{(Eq. 2)}$$

$$\text{DHF} + \text{NADPH} \rightarrow \text{THF} + \text{NADP}^+ \qquad \text{(Eq. 3)}$$

$$\text{Serine} + \text{THF} \rightarrow \text{5,10-CH}_2\text{-THF} + \text{Glycine} \qquad \text{(Eq. 4)}$$

$$\text{5,10-CH}_2\text{-THF} + \text{NADP}^+ \rightarrow \text{5,10-CH}^+\text{-THF} + \text{NADPH} \qquad \text{(Eq. 5)}$$

Conversion of folyl polyglutamates to their monoglutamate forms was achieved by incubation of extracts with

GGH (1 $\mu$L of recombinant zebrafish GGH [4 $\mu$g/$\mu$L] was added to 100 to 200 $\mu$L of extract in a 1.5 mL centrifuge tube). Tubes were flushed with nitrogen gas before capping, incubated at 37°C for 5 min, boiled for 3 min to stop the enzymatic reaction and then immediately cooled on ice. A time study showed that the triglutamate of 5-CHO-THF and the pentaglutamate of methotrexate were converted to their monoglutamate forms in 3 min under these conditions.[17]

After centrifugation and filtration to remove precipitated protein, 50 $\mu$L of the clear supernatant was injected into an Aquasil $C_{18}$ column, 150 × 4.6 mm, 3 $\mu$m (Thermo Electron Corporation) on an HPLC system (Agilent 1100) equipped with fluorescence detector ($\lambda_{ex}$ = 290 nm and $\lambda_{em}$ = 360 nm) for folate analysis. Solvent A was 30 mM phosphoric acid, pH 2.3, and Solvent B was acetonitrile. HPLC was performed as previously described with modification.[19,20] Briefly, the column was equilibrated with 6% solvent B (94% solvent A). After sample injection, the 6% solvent B was maintained for 5 min and then over the next 20 min solvent B was linearly increased to 25% and held at this level for an additional 2 min. Then the solvent composition was decreased to 6% solvent B in 1 min and the column equilibrated for an additional 20 min before the next sample injection. The flow rate was 0.4 mL/min. The potential folate peaks in extracts were identified by overlapping the retention times between the prospective folate peaks and folate standards.

Under the pH conditions used to homogenize tissue samples and HPLC analysis, 5,10-$CH_2$-THF is converted nonenzymatically to THF by dissociation of the methylene group as formaldehyde.[21] This will result in overlapping of signals corresponding to THF and 5,10-$CH_2$-THF. The peak at 18.7 min was confirmed to be THF by its disappearance upon incubating with 6 $\mu$g of SHMT, 100 mM serine, and 3 $\mu$g of MTD, which converts both THF and 5,10-$CH_2$-THF to 5,10-$CH^+$-THF (Eqs. 4 and 5).

The content of THF and 5-$CH_3$-THF were determined directly from chromatograms based on the interpolation of a standard curve. The conversion of DHF to THF was accomplished by adding GGH and 3 $\mu$g DHFR to extracts (Eq. 3) and incubating at 37°C for 5 min. Quantification for DHF was based on the increase in the THF peak area. Analysis of 10-CHO-THF is complicated by the reversible nonenzymatic inter-conversion to 5,10-$CH^+$-THF in acidic solutions.[22,23] Above neutral pH, the equilibrium lies far toward 10-CHO-THF, but below pH 5 it lies far toward 5,10-$CH^+$-THF. To convert these two compounds to THF, controls and extracts were incubated at 37°C for 5 min simultaneously with GGH and 5 $\mu$g FDH-N (Eq. 2). A complicating factor was the observation that adding FDH-N resulted in a ~30% to 70% decrease in the THF peak in standards that contained only THF. The amount of the decrease was dependent on the level of THF and the amount of FDH-N added. To correct for this problem we added to our samples a constant amount of FDH-N and pure THF to a concentration of 120 nM before enzymatic conversion of 10-CHO-THF to THF. Under these conditions, the response of 10-CHO-THF standards was linear with a ~90% recovery rate (Fig. 2). Quantification for 10-CHO-THF was based on the increase in the THF peak area.

### *Characterization of tissue development*

Histochemical analysis on the chemical treated larvae was performed following the protocols described in the Zebrafish book.[24] In brief, anesthetized larvae were fixed in 4% paraformaldehyde, soaked in 30% sucrose and embedded in OCT. Sections of 8 to 10 nm were prepared on a Thermo Scientific Shandon Cryostat 0620E and stained with hematoxyline & eosinophil solutions for pathological examination. Whole-mount *in situ* hybridization (WISH) was performed following the standard protocol described by Jowett and Thisse *et al.*[25,26] Plasmids containing cDNA specific to rhombomere (*krox20*), floor plate (*shh*), mid-hindbrain boundary (*pax2a*) and notochord (*ntl*) (generous gifts from Dr. Jen-Ning Tsai at Chun-Shan Medical University) were linearized with appropriate restriction enzymes. Digoxigenin-UTP-labeled antisense RNA probes were synthesized by *in vitro* transcription with DIG-RNA Labeling kit (SP6/T7) (Roche) and used for *in situ* hybridization. Embryos were placed in glycerol and observed under a dissecting microscope and photographed.

## Results

### *Development and validation of folate detection method with HPLC*

Folate standards. For the purposes of peak identification and quantification, as well as to validate the newly developed HPLC protocol for folate measurement, we analyzed each folate standard of known concentration individually on the same $C_{18}$ reverse phase column that we would use for later analysis. These folate standards were also combined and injected to the same column simultaneously for monitoring the resolution between different folate derivatives. Most of the folate derivatives can be clearly distinguished from each other in HPLC chromatogram (Fig. 2A and Table 1). However, the sensitivity and linear range vary significantly depending on the optical properties of folate derivatives. Highest sensitivity was observed for THF and 5-$CH_3$-THF, since these two folates emit strong fluorescence. Quantification for THF and 5-$CH_3$-THF can be directly obtained by interpolation of the standard curve, in which the peak areas were strongly correlated to the expected concentrations ($r^2$ = 0.999) (Fig. 2B).

Folate derivatives without strong fluorescence, including DHF and 10-CHO-THF, were undetectable in most biological samples, most likely due to their lability and low extinction coefficient. To solve these problems, we added folate enzymes to the extracts to convert these folates to THF, which emits strong fluorescence. The purposes are two-fold: to enhance the signal for detection and to confirm the identity of folate peaks. By adding purified DHFR and NADPH to the reactions, we were able to convert DHF to the highly fluorescent THF (Eq. 3). This allows DHF to become detectable in low nM range (2.5 nM) even in embryos homogenate (data not shown). The content of DHF was calculated from the increased THF peak area ($A_{\text{after DHFR conversion}} - A_{\text{without DHFR conversion}}$) with THF standard curve in the presence of DHFR (Table 2). The linear range of 0.6 to 6.0 pmole for DHF assessment is sufficient to cover DHF concentrations in cells and tissues.[27]

The measurement for 10-CHO-THF appeared to be more complicated than other folate derivatives. We added FDH-N to the cell extracts to convert 10-CHO-THF to THF (Eq. 2). Supposedly, the difference in the THF peak area of samples with/without incubating with FDH-N represents the amount of the converted 10-CHO-THF. Unexpectedly, we found that the change in the THF peak area did not directly reflect the

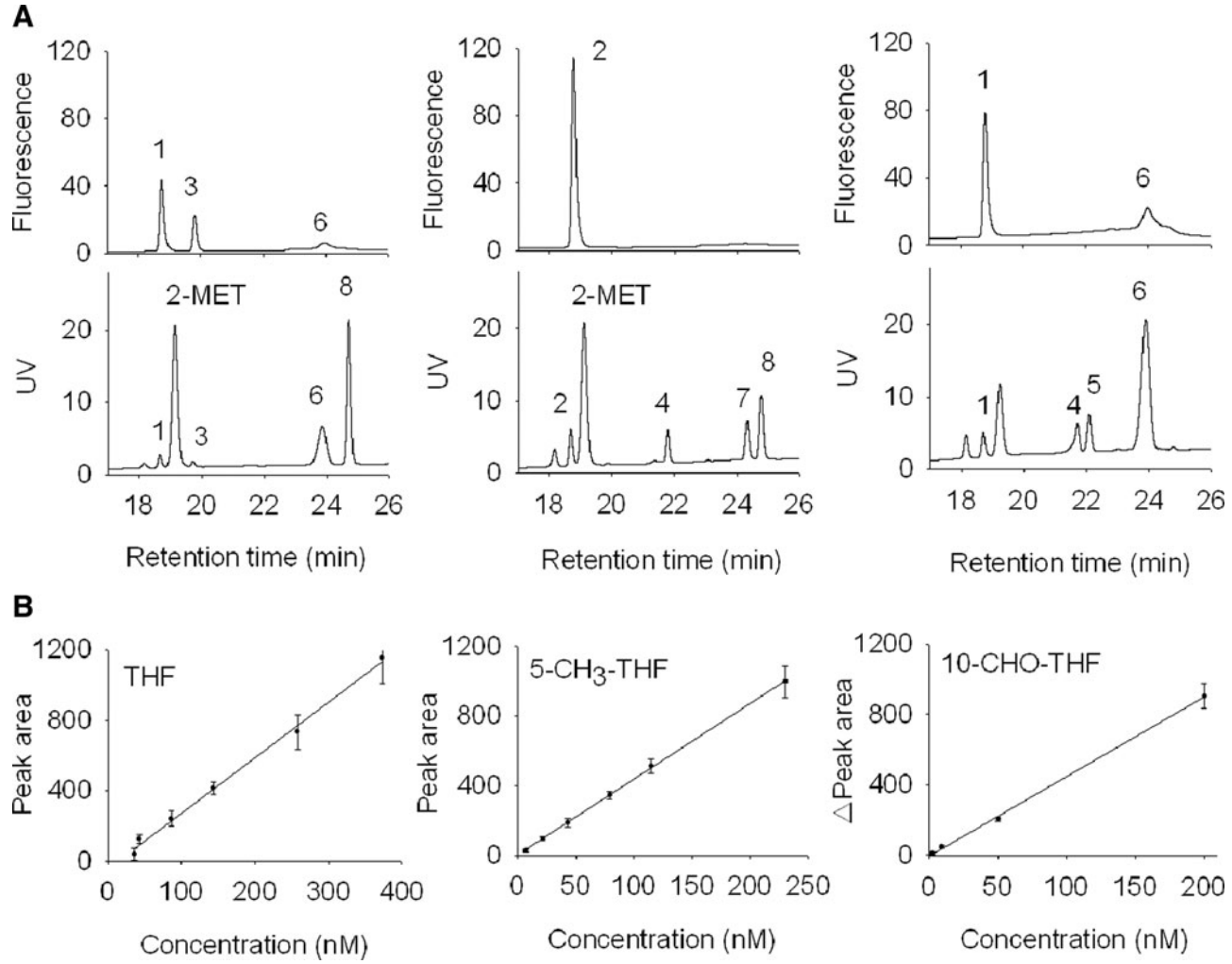


**FIG. 2.** Representative HPLC chromatograms and standard curves of folates. **(A)** Folate monoglutamates of known concentrations in a standard mixture were analyzed on a $C_{18}$-reversed phase column on an Agellient HPLC equipped with both absorbance and fluorescence detectors. Peak 1, THF; 2, 5,10-$CH_2$-THF/THF (This peak was obtained when 5,10-$CH_2$-THF was dissolved in buffer and injected into HPLC column for analysis); 3, 5-$CH_3$-THF, 4, 5,10-$CH^+$-THF; 5, 10-CHO-THF; 6, 5-CHO-THF; 7, DHF; 8, folic acid. The folate concentration represented by each peak is shown in Table 2. **(B)** The standard curves show the linearity between folate concentrations and corresponding peak areas. The regression line for 10-CHO-THF represents the correlation between the change of the THF peak area and the 10-CHO-THF concentration in samples, where the THF concentration is maintained at 120 nM. This standard curve has been corrected for the decrease in the THF area as a result of the addition of FDH-N as described in Materials and Methods. DHF, dihydrofolate; 5-$CH_3$-THF, 5-methyl-tetrahydrofolate; 5,10-$CH_2$-THF, 5,10-methylene-tetrahydrofolate; 10-CHO-THF, 10-formyl-tetrahydrofolate.

amount of 10-CHO-THF added in standard tests. It appeared that the measured 10-CHO-THF concentration varied in accordance with the concentration of pre-existing THF in the sample even when a constant amount of FDH-N was used. To solve this problem and accommodate the range of THF pre-existing in various samples, we brought the final THF concentration of the sample to 120 nM by adding pure THF before adding FDH-N (Supplementary Fig. S1). A standard curve was then constructed by adding increasing amounts of 10-CHO-THF to these samples and calculating the increased THF peak area. This gave a standard linear curve relating the change of THF peak area to 10-CHO-THF concentration (Fig. 2B). The reason for choosing 120 nM is because this concentration would be higher than the endogenous THF concentrations in most biological samples and can be easily reached by adding the required amount of pure THF to each sample.

Validation of the measurements for all examined folate compounds was accomplished by adding known amounts of pure folate derivatives, including DHF and 10-CHO-THF, to zebrafish embryo homogenates before the step of enzymatic conversion, and then comparing the measured results with the expected values. Our results showed that the recovery rates were ~90% or higher for most of the measured folate adducts. Also, the amount of added folate compounds could be faithfully reflected by the change in THF peak area with this protocol and the established standard curves since the measured and expected values were strongly correlated (Table 2 and Supplementary Fig. S2).

It should be noted that most of the 5,10-$CH_2$-THF in samples would be spontaneously converted to THF in the buffer condition used to extract folate. Therefore, THF and 5,10-$CH_2$-THF in embryo extracts remain undistinguishable and are

Table 1. The Optical and Chromatographic Properties of Folate Standards

| *Peak* | *Folate* | *Concentration*[a] *(pmole)* | *Fluorescence (360 nm)* | *UV (290 nm)* | *Retention time (min)* |
|---|---|---|---|---|---|
| 1 | THF | 7.2/12.6 | + | + | 18.7 |
| 2 | 5,10-$CH_2$-THF | 11 | NA[b] | NA[b] | NA[b] |
| 3 | 5-$CH_3$-HF | 2.2 | + | + | 19.8 |
| 4 | 5,10-$CH^+$-THF | 46[c]/54 | – | + | 21.7 |
| 5 | 10-CHO-THF | 34[d] | – | + | 22.0 |
| 6 | 5-CHO-THF | 23/84 | + | + | 23.8 |
| 7 | DHF | 120 | – | + | 24.4 |
| 8 | Folic acid | 50/20 | – | + | 24.7 |

[a]Those showing two concentrations represent the two peaks present in Figure 2A panels 1 and 3 for the same folate adduct (with the same peak number).
[b]Not available. This is because 5,10-$CH_2$-THF was most likely converted to THF in the acidic conditions during chromatography.
[c]This 5,10-$CH^+$-THF was generated from 10-CHO-THF during chromatography in acidic solution.
[d]This concentration was obtained by subtracting the concentration of 5,10-$CH^+$-THF generated during chromatography (b) from the concentration of 10-CHO-THF originally prepared (80 pmole).
DHF, dihydrofolate; 5-$CH_3$-THF, 5-methyl-tetrahydrofolate; 5,10-$CH_2$-THF, 5,10-methylene-tetrahydrofolate; 10-CHO-THF, 10-formyl-tetrahydrofolate.

reported as THF in this study. Nevertheless, combining use of both SHMT and MTD in the extracts allows us to confirm the peak identity for THF/5,10-$CH_2$-THF and distinguish it from other materials that have similar optical properties and elution time on HPLC.

### *Folate composition in zebrafish embryos*

With the developed protocols, we assessed the folate content in the zebrafish embryos of 1 day-postfertilization (dpf). Adding GGH to the extract, separated the potential folates into three distinguishable peaks (Fig. 3A, B). The retention time of peak 1 overlapped with the THF standard. Adding SHMT and MTD to the extracts (which converts THF/5,10-$CH_2$-THF to 5,10-$CH^+$-THF) resulted in disappearance of peak 1, confirming the THF identity of peak 1 (Fig. 3C). The THF peak was significantly increased when DHFR or FDH-N was added to the extract, indicating the conversion of DHF and 10-CHO-THF, respectively, to THF (Fig. 3D, E). We also compared the extraction efficiency for folates for the sample heating time (3–20 min) and with/without pronase digestion as used in other protocols.[28] Extending the heating time in boiling water led to loss of folate in a time-dependent manner. An approximate 50% decrease was observed for DHF when the heating time was extended from 5 to 20 min. The only exception was 5-$CH_3$-THF, which showed no significant loss after heating for 20 min (Supplementary Fig. S3A). Predigestion with pronase did not significantly improve the extraction efficiency but drastically increased the background noise, hindering the detection of folates (Supplementary Fig. S3B). Therefore, the step of pronase digestion was omitted and the heating time for folate extraction was limited to 5 min in the current protocol.

Table 2. Detection Limit and Linear Range of Folates

| *Folate* | *Detection limit (pmole)*[a] | *Recovery rate (%)*[b] | *Linear range (pmole)*[b] |
|---|---|---|---|
| THF/5,10-$CH_2$-THF | 0.2 | 99.0 ± 9.9 | 0.2–18.6 |
| 5-$CH_3$-THF | 0.2 | 103 ± 16.3 | 0.2–12.5 |
| 10-CHO-THF | 0.12 | 88 ± 12.5 | 0.12–10.2 |
| DHF | 0.5 | 100 ± 15.1 | 0.6–6.0 |

[a]The detection limit refers to the lowest concentration of folate in the 50 $\mu$L sample injected for HPLC analysis.
[b]The recovery rate and linear range were determined when folate standards were added to the supernatant of embryo homogenates before the conversion enzymes were added. The concentrations of the standard folate added are, 2 pmole for THF, 1.5 pmole for 5-$CH_3$-THF, 1.6 pmole for 10-CHO-THF, and 4.5 pmole for DHF.

In developing embryos. Our data show that folate adducts fluctuate significantly and differentially during embryogenesis without changing embryonic total folate content. The total folate content of embryos, determined with a microbiological assay, showed no significant difference at various stages (Fig. 4A). On the other hand, 5-$CH_3$-THF was abundant in the crude extract of unfertilized eggs and decreased quickly when the fertilized eggs started to cleave and the primordial cells started to proliferate and differentiate (Fig. 4B and Supplementary Fig. S4). 5-$CH_3$-THF remained low after 24 hpf till at least 120 hpf. 10-CHO-THF existed in high amount with an estimated concentration of 300 fmole/egg. Upon fertilization, a rapid increase followed by a significant decrease occurred. As the embryos continued to develop after 24 hpf, 10-CHO-THF gradually increased again and remained high and constant in the later stages of development. Both THF and DHF were also detected in unfertilized eggs, but only as a small portion of total folate. DHF level decreased as embryos began to grow and remained low during embryogenesis. On the other hand, THF concentration was increased significantly and became dominant in developing embryos at later stages. It appears that both THF and 10-CHO-THF are dominant in embryos beyond 3-dpf when most of the tissues and organs have differentiated and the body floor plan has been well established. It is interesting to note that this fluctuation in folate composition had completely reversed the ratio between THF and other folate adducts in different stage of embryogenesis. A 20- to 40-fold change in these ratios was observed when the fertilized eggs progressed into developing embryos. For example, the ratios of 5-$CH_3$-THF/THF are 10 in unfertilized eggs and 0.25 in 3 dpf embryos. This drastic change in the ratio between two folate

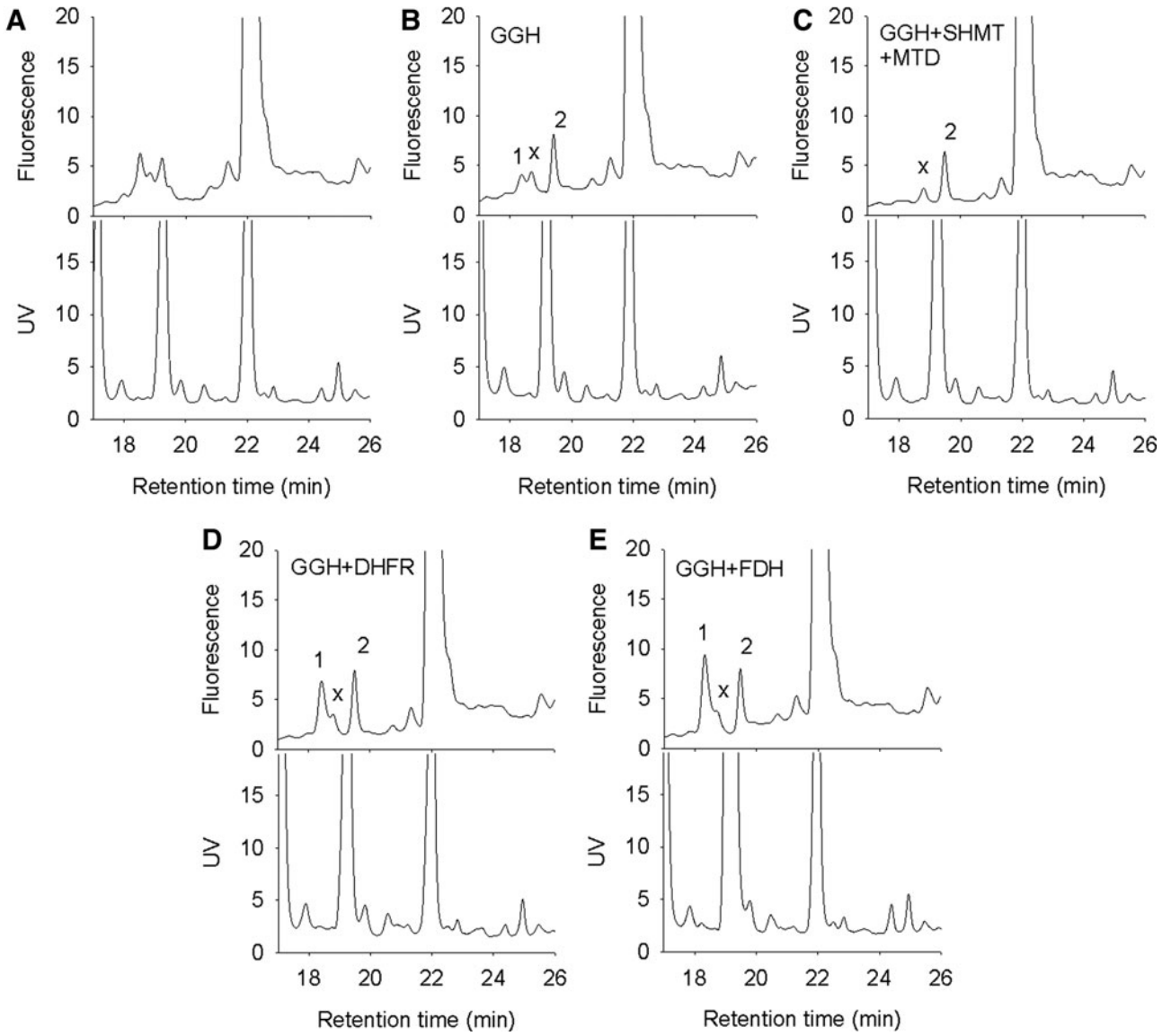


**FIG. 3.** HPLC chromatograms showing the folate content in zebrafish embryos at 1-dpf. Zebrafish embryos at 1-dpf were homogenized and prepared for folate analysis as described in Materials and Methods section. All samples of embryonic extracts were treated with GGH except the one shown in **(A)**. The identity of peak 1 that was observed after GGH treatment **(B)** was confirmed by the disappearance of this peak on incubating the extract with MTD and SHMT **(C)**. Incubating with DHFR **(D)** or FDH-N **(E)** resulted in an increased peak 1 (THF). 10-CHO-THF was determined when the THF concentration in samples was maintained at 120 nM. Peak 1, THF/5,10-$CH_2$-THF; 2, 5-$CH_3$-THF; X, unknown substance. DHFR, dihydrofolate reductase; SHMT, serine hydroxymethyltransferase; dpf, day-postfertilization; MTD, 5,10-methylenetetrahydrofolate dehydrogenase; GGH, $\gamma$-glutamyl hydrolase.

derivatives may alter the activity and property of the folate enzymes that catalyze the corresponding reactions, shift the direction/equilibrium of intracellular one-carbon flow and impede the generation of corresponding metabolites. Our data also show that the combinatory use of folate enzymes enables us to measure the content of folate species that are difficult to detect readily in zebrafish embryonic extracts with conventional methods.

Embryos treated with methotrexate. We found that both embryonic morphology and folate composition were significantly affected by methotrexate. Besides irregular heart development and pericardial edema (data not shown), abnormal neurulation with brain ventricle malformation was observed in 24 hpf embryos when 1 mM methotrexate was added to water at 6 hpf (Fig. 5A, B). Unlike the untreated control group, no clear cranial cavity was formed in the central region of forebrain and midbrain in methotrexate-exposed embryos, implying a disturbed development of diencephalon and hindbrain. Methotrexate-treated embryos were categorized into normal, mild and severe groups based on the severity of the anomaly in brain ventricle formation. More than 80% of embryos exhibited ventricular defects upon exposure to methotrexate. WISH with probes specific to neural tissues also revealed significantly diminished signals for floor plate (*shh*) and mid-hind-brain boundary and spinal cord (*pax2a*) in

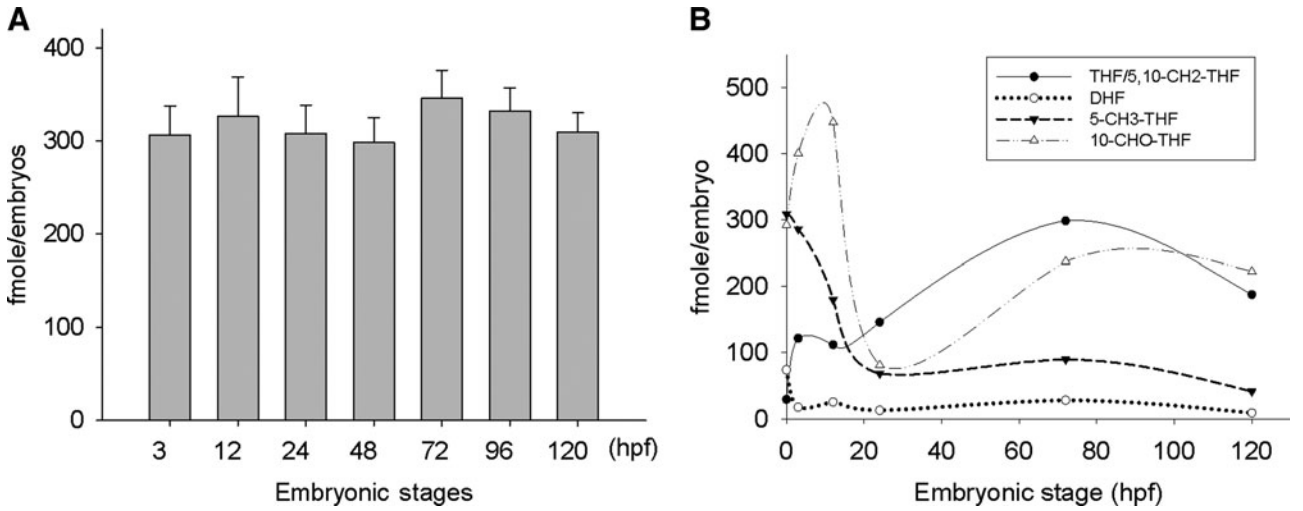


**FIG. 4.** Total folate contents are constant but the folate composition varies significantly in zebrafish embryos of different stages. Zebrafish embryos were collected at indicated stages and subjected to folate extraction and subsequent measurement for total folate **(A)** with a microbiological assay and individual folate adducts **(B)** with HPLC. Data presented are averages of at least three independent repeats with different batches of embryos.

methotrexate-treated embryos although no appreciable difference was observed in the rhombomeres (*krox20*) and notochord (*ntl*) (Fig. 5C and data not shown). Our results show that methotrexate impedes the development of embryonic neural tissues.

As expected, DHF was accumulated and THF was decreased in embryos exposed to methotrexate for 6 h (Fig. 5D). This could be due to the methotrexate-mediated inhibition on DHFR activity. The level of 10-CHO-THF remained largely unchanged. On the other hand, the 5-$CH_3$-THF level was significantly decreased. The extent of this decrease is larger than expected and more significant than that for THF. These results suggest that besides the reduced THF/5,10-$CH_2$-THF, other mechanisms might also contribute to lowering 5-$CH_3$-THF in the presence of methotrexate. We were not able to measure the total folate content of these embryos with microbiological method since the bacteria could not grow in the presence of extracts prepared from methotrexate-treated embryos. This is most likely due to residual methotrexate within the embryos, despite that we had washed these methotrexate-treated embryos thoroughly with fresh water before homogenization for folate extraction.

Embryos cotreated with methotrexate and leucovorin. To evaluate the efficacy of folate supplementation to methotrexate-induced folate deficiency, 10 mM leucovorin was added to embryos water with methotrexate simultaneously. Leucovorin is the folate derivatives commonly used to rescue folate metabolism when methotrexate is employed for clinical therapy. We found that the severity of the defective phenotypes induced by methotrexate was partly alleviated in embryos exposed to both methotrexate and leucovorin simultaneously (Fig. 5A). Both the THF level and the sum of the four measured folate adducts were reversed. The content of 10-CHO-THF was slightly increased. However, the accumulation of DHF and the decrease of 5-$CH_3$-THF remained (Fig. 5D). These results indicate that the methotrexate-induced disturbance in OCM is not completely rescued by leucovorin supplementation although the embryonic total folate content has been restored.

## Discussion

In this study, we report the chronological dynamics of folate metabolites in developing embryos. We also show that methotrexate induces a significant decrease in 5-$CH_3$-THF levels, which cannot be reversed by leucovorin supplementation and is likely to bring a profound and irreversible impact to cellular methylation potential. Epigenetic control is crucial for both cell fate determination during embryogenesis and the development of drug resistance, especially for the regimen involving antifolate therapy.[1,29–31] The current study provides insight to the metabolic control of a dietary nutrient and how it may affect embryonic development and cellular methylation potential.

OCM during embryogenesis. Generally speaking, reduced folate compounds are unstable and easily oxidized. The two most stable reduced folates are 5-CHO-THF and 5-$CH_3$-THF.[32] In unfertilized zebrafish eggs, the primary reduced folates are 5-$CH_3$-THF and 10-CHO-THF (Fig. 4). The presence of a large amount of 5-$CH_3$-THF is understandable because of its stability. Studies with mouse embryos suggest that epigenetic control involving hypomethylation is involved in NTDs.[1,31] Global hypermethylation and hypomethylation in the promoter region of critical genes were also reported for folate deficient animal with neural tissues anomaly.[33] The abundant 5-$CH_3$-THF present in eggs will provide the convenience for the epigenetic control crucial for embryogenesis. The immediate and steep decrease of 5-$CH_3$-THF after fertilization supports the above speculation and echoes the epigenetic role of folate and DNA hypomethylation in embryonic pathogenesis.

The presence of an equally high amount of 10-CHO-THF in eggs is unexpected, since 10-CHO-THF is one of the most labile forms of reduced folates. Nevertheless, the high content

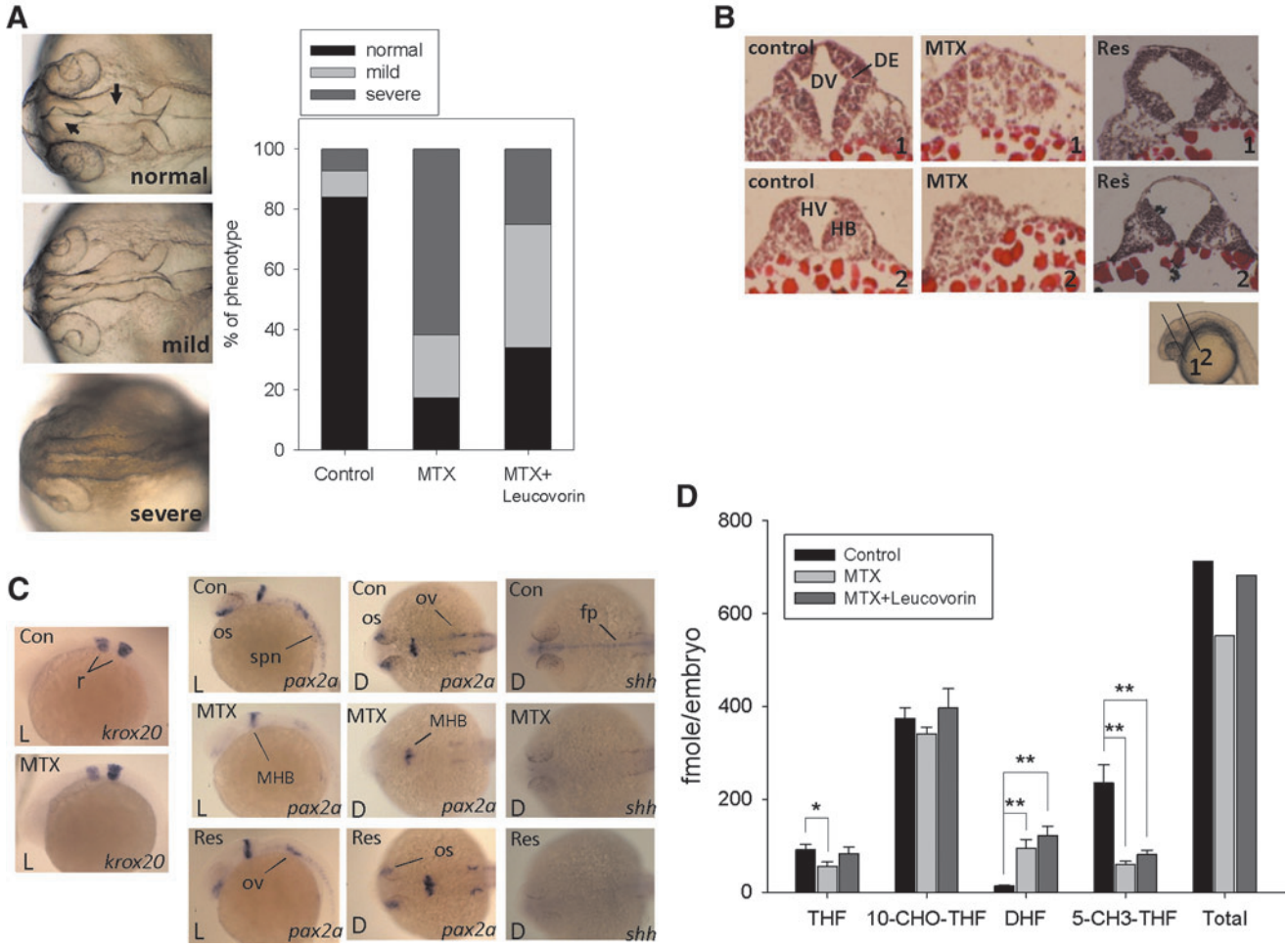


**FIG. 5.** Methotrexate-induced morphological abnormality and altered folate composition in embryos are partly reversed by leucovorin. Methotrexate (with or without leucovorin) was added to the wells containing embryos at 6 hpf to 1.5 mM and collected at indicated time points for characterization. **(A)** Embryos were collected at 24 hpf and evaluated for gross morphology under light a dissecting microscope. Embryonic phenotype is categorized into normal, mild, and severe groups mainly based on brain ventricle formation. A total of ~80 embryos were included for each group in three separate and independent trials. **(B)** Embryos were subjected to cryo-sectioning and HE stain for examining the brain ventricular cavity. *Inset* shows the position of cross-sections. Res, rescue (by adding methotrexate and leucovorin simultaneously); DE, diencephalon; DV, diencephalic ventricle; HB, hindbrain; HV, hindbrain ventricle. **(C)** The development of embryonic neural tissues was characterized at 24 hpf with *in-situ* hybridization using neural tissue specific probes *krox20*(rhombomere), *shh* (floor plate), and *pax2a* (mid-hindbrain boundary and spinal cord); Con, control, embryos without any treatment; MTX, methotrexate treated; Res, rescue; L, lateral view; D, dorsal view; r, rhombomere; os, optical stalk; ov, otic vesicle; spn, spinal cord; MHB, mid-hindbrain boundary; fp, floor plate. **(D)** Embryos were collected at 12 hpf and subjected to folate composition analysis with HPLC. The data presented are the averages of at least three independent experiments with different batches of embryos. "Total" refers to the sum of the four folate adducts examined in the study. $*p < 0.05$, $**p < 0.005$. hpf, hour postfertilization.

of 10-CHO-THF in eggs has the advantage of preserving the carbon source required for subsequent massive purine synthesis for cell proliferation. This is reflected in the steep drop of 10-CHO-THF between 10 and 24 hpf when the fertilized embryos quickly grow in cell number and embryo size. 10-CHO-THF reaches the lowest level at 24 hpf when embryonic body plan is well established. This fluctuation is also in harmony with the change in zebrafish embryonic cell cycle duration at various stages. The accumulation of 10-CHO-THF at later stages is likely to be a result of the shorter cell cycle duration before mid-blastula (15 min/cycle; where nucleotide synthesis is active and lots of 10-CHO-THF is required) followed by the gradually lengthened cell cycle after 24 hpf.[16] Studies in mammals show that some proteins bind labile reduced folates and help stabilize them.[34] The binding of 10-CHO-THF to a protein in unfertilized zebrafish eggs could explain the high abundance of 10-CHO-THF in embryos. We also noticed that the sum of folate adducts were all higher than the total folate measured with microbiological assay of the same stage. This could result from folate being lost during the 24-h incubation time for bacterial growth in the microbiological method. Previous studies showed that in plants and spores the primary reduced folate is 5-CHO-THF, which rapidly converted to other one-carbon adducts in OCM

during early stages of growth.[35] We do not know but cannot exclude the possibility that a significant amount of 5-CHO-THF is also present in zebrafish eggs and embryos due to the limitation of this method.

Effect of methotrexate and leucovorin on embryo development and OCM. Our data suggest that the methotrexate-induced disturbance in OCM might be more substantial to embryonic methylation potential (5-$CH_3$-THF level for SAM production) than to nucleotide synthesis (10-CHO-THF/THF/5,10-$CH_2$-THF for nucleotides synthesis). The crucial role of folate in cell proliferation and differentiation has prompted the development of antifolate drug, such as methotrexate, trimethoprim, pyrimethamine, and pemetrexed. Methotrexate is a chemotherapeutic drug for treating a number of cancers and autoimmune diseases.[36,37] However, the often emerging methotrexate-resistance has impeded its curative potential. Methotrexate works as an antifolate agent, which competitively inhibits the binding of folic acid to DHFR. Therefore, it is not surprising to detect the accumulation of DHF and the decrease of THF in methotrexate-treated embryos.[13] However, that 5-$CH_3$-THF decreases with a magnitude much greater than THF/5,10-$CH_2$-THF decreases is unexpected. One likely explanation for the significant decrease of 5-$CH_3$-THF, besides the lowered THF/5,10-$CH_2$-THF level (the precursor of 5-$CH_3$-THF), is DHF-mediated inhibition on the activity of methylenetetrahydrofolate reductase (MTHFR). MTHFR irreversibly converts 5,10-$CH_2$-THF to 5-$CH_3$-THF.[38] The observation that leucovorin cotreatment did not reverse 5-$CH_3$-THF level supports the above speculation. In fact, further decrease in 5-$CH_3$-THF was even detected occasionally in the cotreated embryos (data not shown). Leucovorin is expected to bypass DHFR and enter the folate pool via the activity of 5,10-$CH^+$-THF synthetase and replenish the reduced folate pool (Fig. 1).[39] This is reflected in the increased levels of THF/5,10-$CH_2$-THF and 10-CHO-THF. However, leucovorin did not relieve the inhibition on DHFR, leading to continuous accumulation of DHF and inhibition on MTHFR. Based on these results and more precisely speaking, the impact of methotrexate on embryonic OCM is better described as OCM "disturbance" or "imbalance" rather than "folate deficiency." Our results imply that cells under the treatment of methotrexate-leucovorin may possess a tolerable ability to proliferate but with higher propensity to undergo transformation via epigenetic control, which might contribute to the occurrence of congenital abnormality and development of drug resistance. We are convinced that this effect shall not be overlooked since high doses of leucovorin are often administrated repeatedly in combination with methotrexate for diseases treatment clinically. Further studies are required to determine whether the "irreversible" decrease of 5-$CH_3$-THF is responsible for the incompletely rescued phenotypes. Investigation on the impact to the epigenetic control of crucial genes and its correlation with the development of methotrexate-resistance is also important, especially for the individuals carrying *MTHFR* polymorphisms.[40] For instance, both C677T (valine substitution) and A1298C (alanine substitution) polymorphisms on *MTHFR* result in a less active enzyme.[41,42] Patients carrying these polymorphisms may be more likely to experience toxicity or develop resistance against methotrexate-leucovorin therapy.

Our findings that methotrexate-exposure causes abnormal brain ventricle formation is the first report on the methotrexate-induced neural malformation in a vertebrate other than mammal, adding further emphasis to the crucial role of folate in neural tissue development. Our results also support the comparability between zebrafish and mammalian OCM, as well as their susceptibility and response to an antifolate drug. In the zebrafish model, abnormal heart formation has been reported in methotrexate-exposed embryos, but never the defects in neural tissues development.[43] The successful, although partial, reverse of abnormal phenotypes with folate supplementation suggests the potential use of methotrexate-treated zebrafish embryos as an *in vivo* platform for studying the etiology and therapeutic regimens for folate-related NTDs.

Analysis of folates. We used HPLC to separate and measure different folate adducts. However, to identify the *in vivo* concentration of natural folates using HPLC is inherently difficult due to the existence of multiple polyglutamyl chain lengths, the variety and instability of reduced folate derivatives, the interference by nonfolate compounds and the low optical activity of some folate adducts. The use of purified GGH in the current protocol allows us to avoid using a large volume of serum or pancreas extract, which often result in significant dilution of samples and high background. It also allows us to avoid the long incubation time required for an acceptable conversion of the polyglutamate to the monoglutamate forms, which results in loss of folates. The conversion of nonfluorescent DHF and 10-CHO-THF to THF with purified folate enzymes aids in peak identification. Although the requirement for purifying the recombinant folate enzymes might be inconvenient, all the enzymes can be purified with one-step/one-column purification protocols within 6 h, since most of these recombinant enzymes are His-tagged. In our experience, ~8 to 15 mg of pure enzymes can be obtained from 1 L of *E. coli* culture, which is sufficient for more than 3000 reactions. In addition, these enzymes are stable when stored at low temperature. Therefore, frequent purification of enzymes is not necessary. Another advantage of using zebrafish GGH to remove the polyglutamate chain is that it is active at pH 10 unlike GGH currently used from mammalian extracts.[17]

## Conclusion

In this study, we developed a new protocol, which allows us to determine the individual folate adducts in zebrafish embryos, especially those with low optical activity. We showed that different folate adducts in one-carbon pools fluctuated chronologically and significantly during embryogenesis and responded differentially to methotrexate-leucovorin treatment. The disturbance caused by methotrexate in folate-mediated OCM was more substantial to the pathways involving in cellular methylation potential than to those for nucleotide synthesis. In addition, the methotrexate-treated zebrafish embryos may serve as an *in vivo* model for studying NTDs caused by folate-mediated OCM impairment.

## Acknowledgments

Our sincere appreciation goes to Dr. Verne Schirch, Virginia Commonwealth University, for his valuable advice and

assistance in editing. We also thank Taiwan Zebrafish Core Facility at ZeTH (supported by NSC grant 101-2321-B-400-014) for the material and technical support. This work was supported by National Science Council, Taiwan (NSC 99-2320-B-006-013-MY3) and the Program for Promoting Academic Excellence of Universities, National Cheng Kung University (D98-3500 [C008]).

### Disclosure Statement

No competing financial interests exist.

### References

1. Shane B. Folate and vitamin B12 metabolism: overview and interaction with riboflavin, vitamin B6, and polymorphisms. Food Nutr Bull 2008;29:S5–S16.
2. Gisondi P, Fantuzzi F, Malerba M, Girolomoni G. Folic acid in general medicine and dermatology. J Dermatol Treat 2007;18:138–146.
3. Troen AM, Mitchell B, Sorensen B, Wener MH, Johnston A, Wood B, *et al.* Unmetabolized folic acid in plasma is associated with reduced natural killer cell cytotoxicity among postmenopausal women. J Nutr 2006;136:189–194.
4. Cole BF, Baron JA, Sandler RS, Haile RW, Ahnen DJ, Bresalier RS, *et al.* Folic acid for the prevention of colorectal adenomas: a randomized clinical trial. JAMA 2007;297:2351–2359.
5. Ciappio ED, Mason JB, Crott JW. Maternal one-carbon nutrient intake and cancer risk in offspring. Nutr Rev 2011;69:561–571.
6. Tibbetts AS, Appling DR. Compartmentalization of Mammalian folate-mediated one-carbon metabolism. Annu Rev Nutr 2010;30:57–81.
7. Herbig K, Chiang EP, Lee LR, Hills J, Shane B, Stover PJ. Cytoplasmic serine hydroxymethyltransferase mediates competition between folate-dependent deoxyribonucleotide and S-adenosylmethionine biosyntheses. J Biol Chem 2002;277:38381–38389.
8. Anguera MC, Field MS, Perry C, Ghandour H, Chiang EP, Selhub J, *et al.* Regulation of folate-mediated one-carbon metabolism by 10-formyltetrahydrofolate dehydrogenase. J Biol Chem 2006;281:18335–18342.
9. Kari G, Rodeck U, Dicker AP. Zebrafish: an emerging model system for human disease and drug discovery. Clin Pharmacol Ther 2007;82:70–80.
10. Chang WN, Tsai JN, Chen BH, Fu TF. Cloning, expression, purification, and characterization of zebrafish cytosolic serine hydroxymethyltransferase. Protein Expr Purif 2006;46:212–220.
11. Chang WN, Tsai JN, Chen BH, Huang HS, Fu TF. Serine hydroxymethyltransferase isoforms are differentially inhibited by leucovorin-Characterization and comparison of recombinant zebrafish serine hydroxymethyltransferases. Drug Metab Dispos 2007;35:2127–2137.
12. Chang WN, Lin HC, Fu TF. Zebrafish 10-formyltetrahydrofolate dehydrogenase is similar to its mammalian isozymes for its structural and catalytic properties. Protein Expr Purif 2010;72:217–222.
13. Kao TT, Wang KC, Chang WN, Lin CY, Chen BH, Wu HL, *et al.* Characterization and comparative studies of zebrafish and human recombinant dihydrofolate reductases—inhibition by folic acid and polyphenols. Drug Metab Dispos 2008;36:508–516.
14. Stover P, Schirch V. Synthesis of (6S)-5-formyltetrahydropteroylpolyglutamates and interconversion to other reduced pteroylpolyglutamate derivatives. Anal Biochem 1992;202:82–88.
15. Westerfield M. The Zebrafish Book: Guide for the Laboratory Use of Zebrafish *(Danio rerio)*. Eugene: University of Oregon Press, 4th Edition, 2000.
16. Kimmel CB, Ballard WW, Kimmel SR, Ullmann B, Schilling TF. Stages of embryonic development of the zebrafish. Dev Dyn 1995;203:253–310.
17. Kao TT, Chang WN, Wu HL, Shi GY, Fu TF. Recombinant zebrafish {gamma}-glutamyl hydrolase exhibits properties and catalytic activities comparable with those of mammalian enzyme. Drug Metab Dispos 2009;37:302–309.
18. Fu TF, di Salvo M, Schirch V. Enzymatic determination of homocysteine in cell extracts. Anal Biochem 2001;290:359–365.
19. Kao TT, Tu HC, Chang WN, Chen BH, Shi YY, Chang TC, *et al.* Grape seed extract inhibits the growth and pathogenicity of Staphylococcus aureus by interfering with dihydrofolate reductase activity and folate-mediated one-carbon metabolism. Int J Food Microbiol 2010;141:17–27.
20. Patring JD, Jastrebova JA, Hjortmo SB, Andlid TA, Jagerstad IM. Development of a simplified method for the determination of folates in baker's yeast by HPLC with ultraviolet and fluorescence detection. J Agric Food Chem 2005;53:2406–2411.
21. Horne DW. High-performance liquid chromatographic measurement of 5,10-methylenetetrahydrofolate in liver. Anal Biochem 2001;297:154–159.
22. Tabor H, Wyngarden L. The enzymatic formation of formiminotetrahydrofolic acid, 5,10-methenyltetrahydrofolic acid, and 10-formyltetrahydrofolic acid in the metabolism of formiminoglutamic acid. J Biol Chem 1959;234:1830–1846.
23. Baggott JE. Hydrolysis of 5,10-methenyltetrahydrofolate to 5-formyltetrahydrofolate at pH 2.5 to 4.5. Biochemistry 2000;39:14647–14653.
24. Westerfield M. The Zebrafish Book: Guide for the Laboratory Use of Zebrafish *(Danio rerio)*. Eugene: University of Oregon Press, 5th Edition, 2007.
25. Jowett T. Double *in situ* hybridization techniques in zebrafish. Methods 2001;23:345–358.
26. Thisse C, Thisse B, Schilling TF, Postlethwait JH. Structure of the zebrafish snail1 gene and its expression in wild-type, spadetail and no tail mutant embryos. Development 1993;119:1203–1215.
27. Glauner H, Ruttekolk IR, Hansen K, Steemers B, Chung YD, Becker F, *et al.* Simultaneous detection of intracellular target and off-target binding of small molecule cancer drugs at nanomolar concentrations. Br J Pharmacol 2010;160:958–970.
28. Arcot J, Shrestha A. Folate: methods of analysis. Trends Food Sci Technol 2005;16:253–266.
29. Shoemaker RH. Genetic and epigenetic factors in anticancer drug resistance. J Natl Cancer Inst 2000;92:4–5.
30. Yu W, Jin C, Lou X, Han X, Li L, He Y, *et al.* Global analysis of DNA methylation by Methyl-Capture sequencing reveals epigenetic control of cisplatin resistance in ovarian cancer cell. PLoS One 2011;6:e29450.
31. Burren KA, Savery D, Massa V, Kok RM, Scott JM, Blom HJ, *et al.* Gene-environment interactions in the causation of neural tube defects: folate deficiency increases susceptibility conferred by loss of Pax3 function. Hum Mol Genet 2008;17:3675–3685.
32. Forssen KM, Jagerstad MI, Wigertz K, Witthoft CM. Folates and dairy products: a critical update. J Am Coll Nutr 2000;19:100S–110S.

33. Friso S, Choi SW, Girelli D, Mason JB, Dolnikowski GG, Bagley PJ, *et al.* A common mutation in the 5,10-methylenetetrahydrofolate reductase gene affects genomic DNA methylation through an interaction with folate status. Proc Natl Acad Sci U S A 2002;99:5606–5611.
34. Fu TF, Maras B, Barra D, Schirch V. A noncatalytic tetrahydrofolate tight binding site is on the small domain of 10-formyltetrahydrofolate dehydrogenase. Arch Biochem Biophys 1999;367:161–166.
35. Kruschwitz HL, McDonald D, Cossins EA, Schirch V. 5-Formyltetrahydropteroylpolyglutamates are the major folate derivatives in Neurospora crassa conidiospores. J Biol Chem 1994;269:28757–28763.
36. Hyoun SC, Obican SG, Scialli AR. Teratogen update: methotrexate. Birth Defects Res A Clin Mol Teratol 2012;94:187–207.
37. Skubisz MM, Tong S. The evolution of methotrexate as a treatment for ectopic pregnancy and gestational trophoblastic neoplasia: a review. ISRN Obstet Gynecol 2012;2012:637094.
38. Matthews RG, Daubner SC. Modulation of methylenetetrahydrofolate reductase activity by S-adenosylmethionine and by dihydrofolate and its polyglutamate analogues. Adv Enzyme Regul 1982;20:123–131.
39. Huang T, Schirch V. Mechanism for the coupling of ATP hydrolysis to the conversion of 5-formyltetrahydrofolate to 5,10-methenyltetrahydrofolate. J Biol Chem 1995;270:22296–22300.
40. Porcelli L, Assaraf YG, Azzariti A, Paradiso A, Jansen G, Peters GJ. The impact of folate status on the efficacy of colorectal cancer treatment. Curr Drug Metab 2011;12:975–984.
41. Weisberg I, Tran P, Christensen B, Sibani S, Rozen R. A second genetic polymorphism in methylenetetrahydrofolate reductase (MTHFR) associated with decreased enzyme activity. Mol Genet Metab 1998;64:169–172.
42. Goyette P, Rozen R. The thermolabile variant 677C→T can further reduce activity when expressed in cis with severe mutations for human methylenetetrahydrofolate reductase. Hum Mutat 2000;16:132–138.
43. Sun S, Gui Y, Wang Y, Qian L, Liu X, Jiang Q, *et al.* Effects of methotrexate on the developments of heart and vessel in zebrafish. Acta Biochim Biophys Sin (Shanghai) 2009;41:86–96.

Address correspondence to:
*Tzu-Fun Fu, PhD*
*Department of Medical Laboratory Science and Biotechnology*
*National Cheng Kung University*
*College of Medicine*
*No.1, University Road*
*Tainan 701*
*Taiwan*

*E-mail:* tffu@mail.ncku.edu.tw